Geophysical Research Letters

Supporting Information for

Accelerated Recent Warming and Temperature Variability over the Past Eight Centuries in the Central Asian Altai from Blue Intensity in Tree Rings

N. K. Davi[1,2], M. P. Rao[2,3], R. Wilson[2,4], L. Andreu-Hayles[2], R. Oelkers[2,5], R. D'Arrigo[2], B. Nachin[2,6], B. Buckley[2], N. Pederson[7], C. Leland[2], & B. Suran[8]

[1]Dept. of Environmental Science, William Paterson University, Wayne, NJ, 07470, U.S.A., [2]Tree-Ring Laboratory, Lamont-Doherty Earth Observatory of Columbia University, Palisades, NY, 10964, U.S.A., [3]Cooperative Programs for the Advancement of Earth System Science, University Corporation for Atmospheric Research, Boulder, CO 80307, U.S.A., [4]School of Earth and Environmental Sciences, University of St Andrews, Scotland KY16 9AJ, U.K., [5]Dept. of Earth and Environmental Science, Columbia University, NY, 10027, U.S.A., [6]Graduate School, National University of Mongolia, 14201 Ulaanbaatar, Mongolia, [7]Harvard Forest, Harvard University, Petersham, MA 01366, U.S.A., [8]Department of Environment and Forest Engineering, School of Engineering & Applied Sciences, National, University of Mongolia, Ulaanbaatar 14201, Mongolia

Contents of this file

Introduction

The supporting information contains additional text for the introduction section, the nine supporting figures mentioned in the main text, and three supporting table referenced in the main text.

Text S1. Main site features were described by the late Gordon Jacoby from his expedition in 2005: '*The woodlands were widely-spaced and open-canopied, with alpine vegetation growing between the trees. Competition between trees thus appeared to be a minimal limiting factor to*

growth. There were small rivulets of water through and above this treeline indicating sufficient access to water. Therefore, considering the high elevation of the site, tree growth was hypothesized to be limited by temperature rather than moisture. At BU, cross sections from relict logs that died centuries ago were also collected." A video description of the site can be found here: Nicole K. Davi, January 4th, 2021, Bairam Uul Tree-Ring Site [Video] Youtube. https://youtu.be/-FyRoqIaHsM). Cores were taken from living trees along a traverse of the upper forest border and sections from dead trees were obtained in the same vicinity.

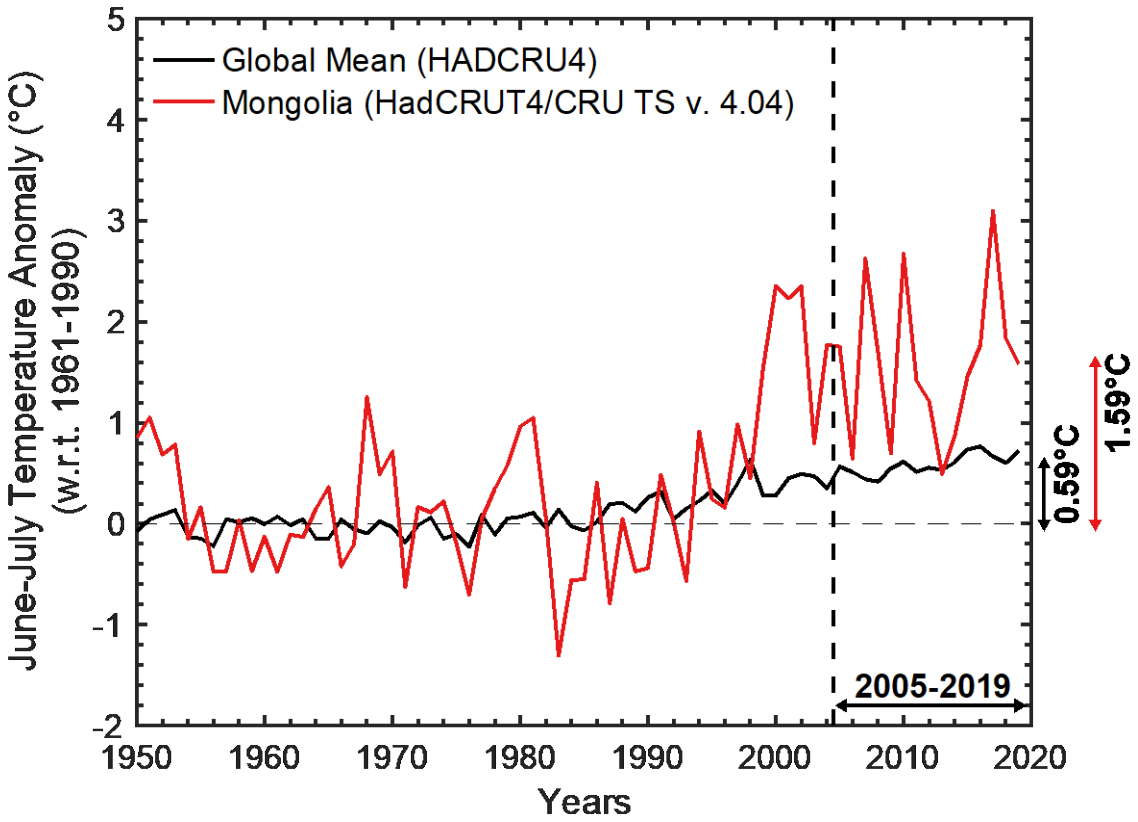

Figure S1. Global mean (in black) and Western Mongolia (86-94.5°E, 46.5-52°N, in red) June-July temperature anomalies since 1950 C.E. relative to 1961-1990 C.E. The temperature data are from the HADCRU4 global gridded temperature dataset (Morice et al., 2012). Mean temperature anomalies were calculated after weighting each grid-cell by the cosine of its latitude. This accounts for the decrease in the spatial extent of grid-cells as we move from the equator to a point of singularity at the poles (Jones & Hulme, 1996). Mean warming between 2005-2019 C.E. relative to 1961-1990 C.E is 0.59°C globally and 1.59°C for Mongolian June-July temperature.

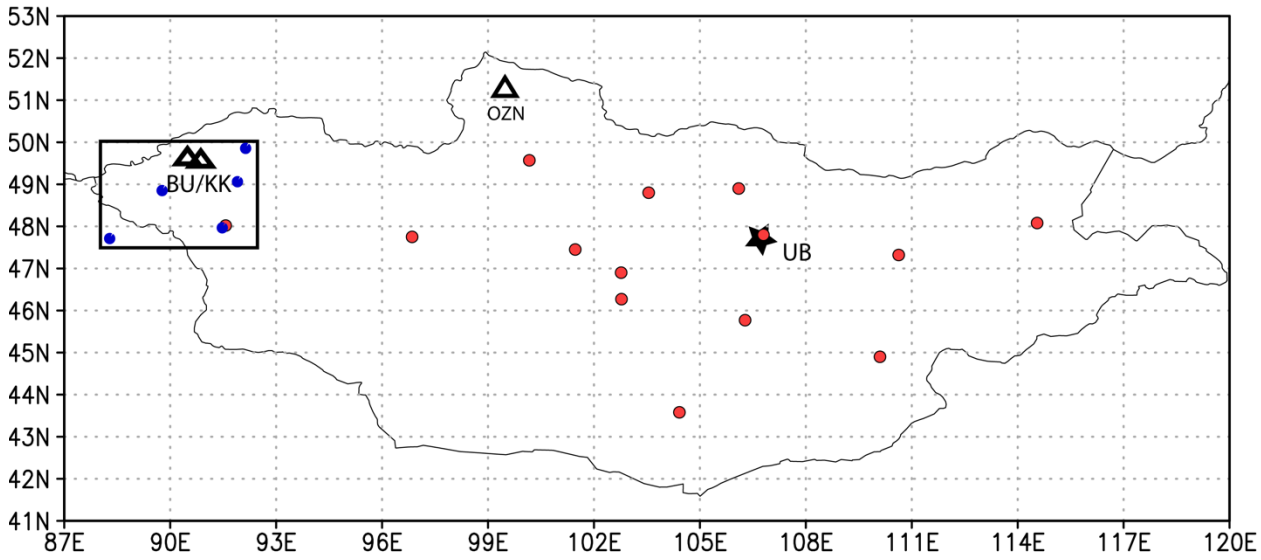

Figure S2. Map of Mongolia showing the location of the tree-ring sites (triangles) Bairam Uul (BU), Khalzan Khamar (KK), and Ondor Zuun Nuruu (OZN, Davi et al., 2015), GHCN temperature station records that span at least 1950-2019 (red dots), Ulaanbatar (UB, star), the capital of Mongolia, nearest station records (blue dots), and the area used to develop regionalized CRU data for western Mongolia (rectangle). From west to east the nearest stations (blue dots) are Altay, Uigi, Hovd, Omno-Gobi, and Bayan-Ol.

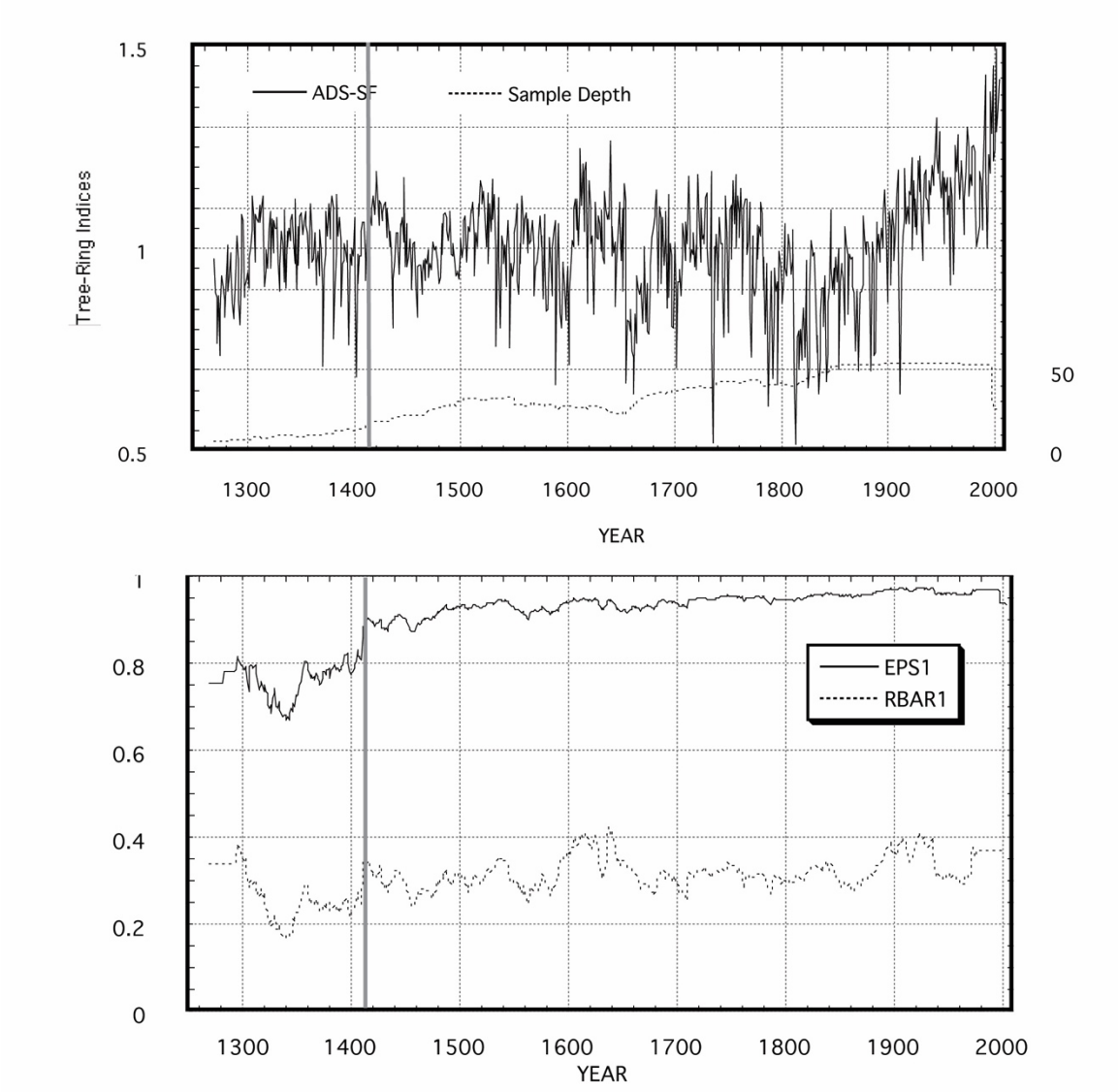

Figure S3. Tree-ring ADS-SF chronology and sample size (top), and running EPS and running Rbar (bottom). The vertical bar shows when EPS reaches 0.85.

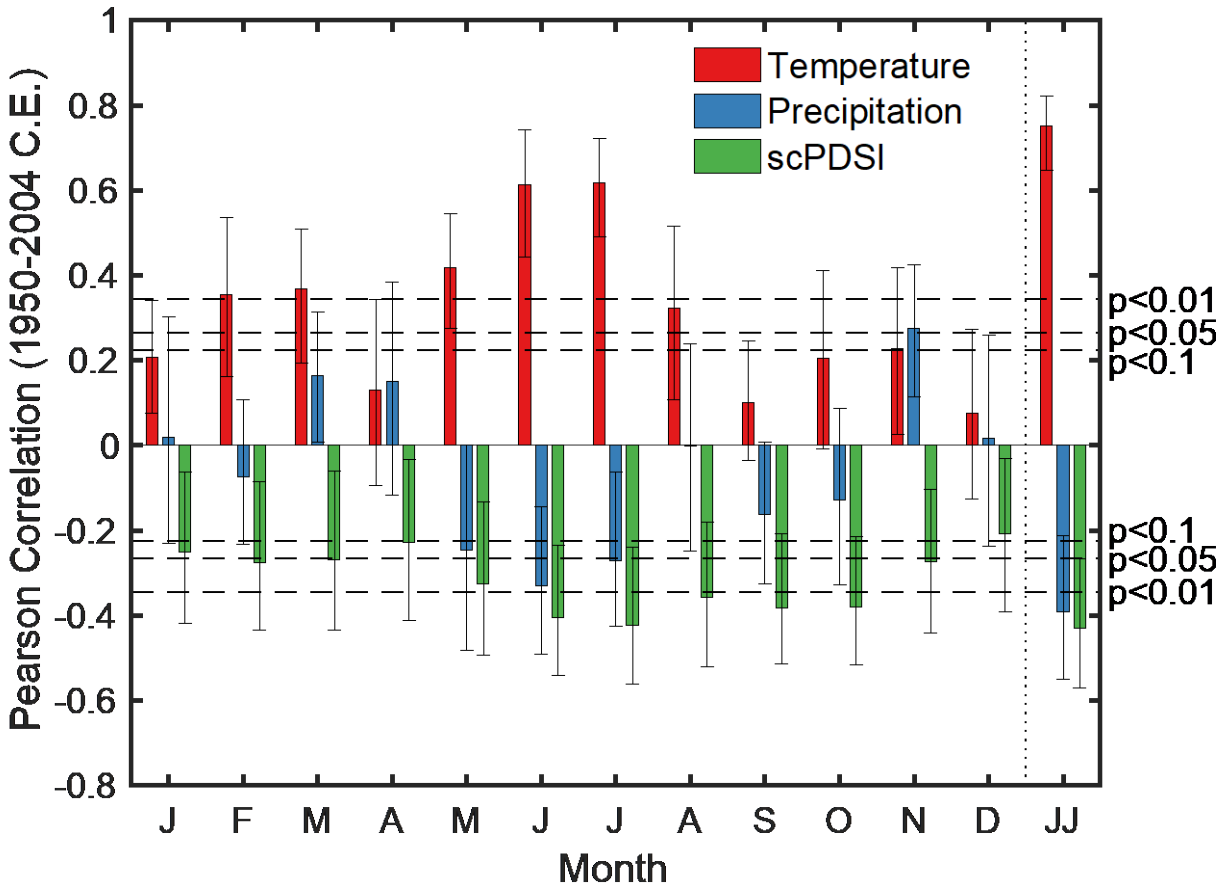

Figure S4 Monthly correlation response function plots for the age dependent spline with signal free (ADS-SF) delta blue intensity (DBI) chronology against regional temperature (in red), precipitation (in blue), and scPDSI (in green) between 1950-2004 C.E. Temperature and precipitation from CRU Ts v. 4.04 (Harris et al., 2020), and scPDSI is from van der Schrier et al., (2013). Climate data are averaged between 88-92.5°E and 47.5-50°N. scPDSI - Self-calibrating Palmer Drought Severity Index. The strongest significant positive correlation for the ADS-SF chronology is for June and July temperatures. The correlation between the ADS-SF and mean June-July (JJ) climate is shown in the final column on the right. The other three standardized chronology variants (2GR-RCS-SF, 2GR-RCS-SF, and 3GR-RCS-TRAD) show nearly identical responses.

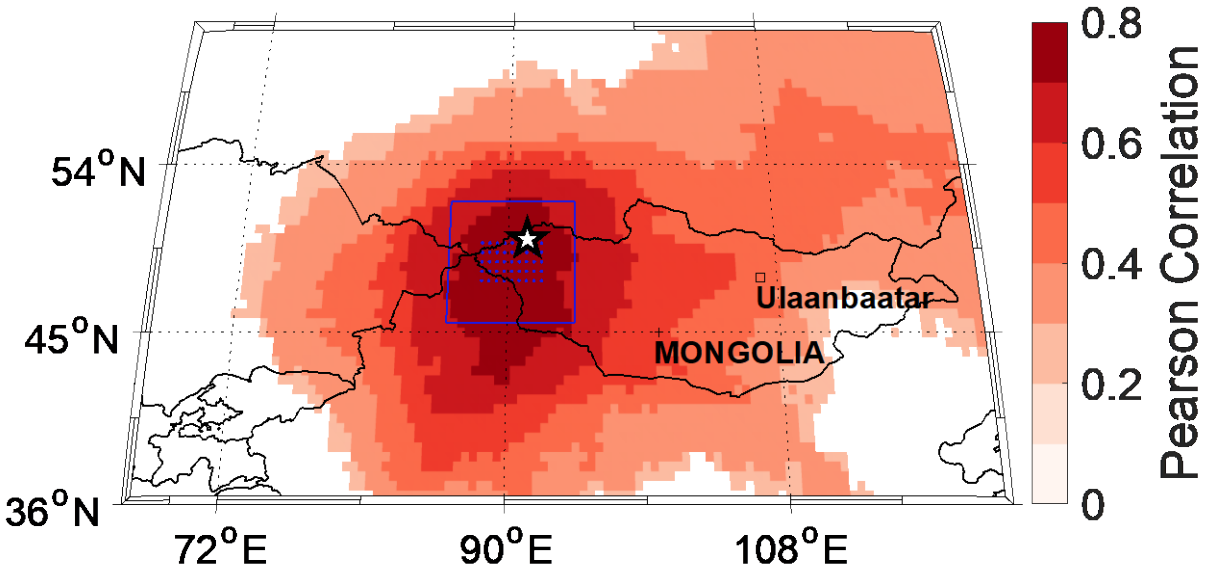

Figure S5. Same as Figure 3 of the main text but for the spatial correlation between our ADS-SF BUKK mean June-July temperature DBI reconstruction and CRU TS v. 4.04 mean June-July temperature between 1950-2004 without first-differencing either series.

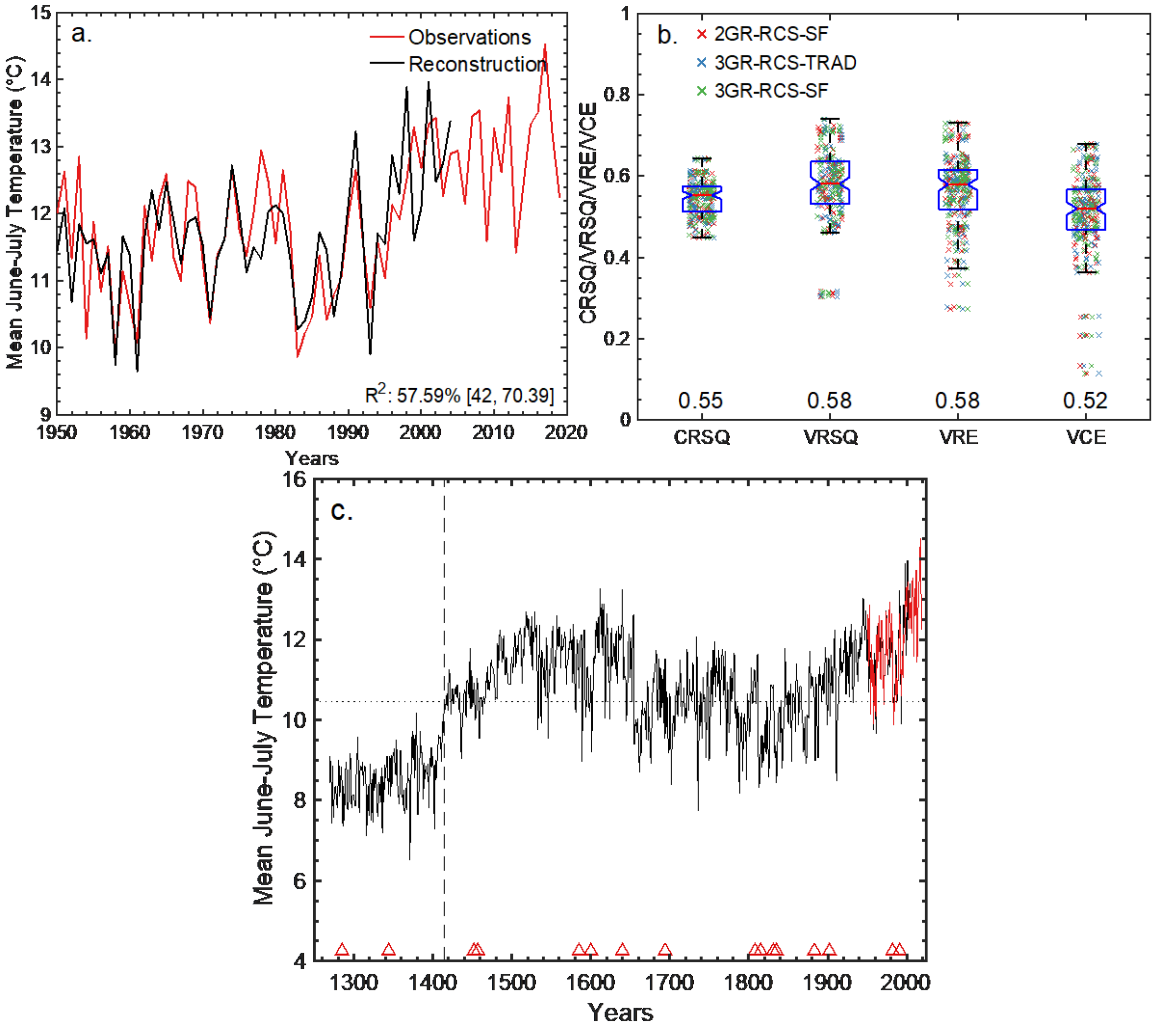

Figure S6. Instrumental observations (in red) and the delta blue intensity (DBI) RCS-COMP reconstruction (in black) of mean June-July (JJ) summer temperatures for Western Mongolia [88-92.5°E, 47.5-50°N]. The RCS-COM reconstruction is calculated as the median of the 3 RCS reconstructions (2GR-RCS-SF, 3GR-RCS-TRAD, and 3GR-RCS-SF) while its associated uncertainties are derived from the widest possible uncertainty range of the three RCS reconstructions. **(a.)** Comparison between instrumental observations and our reconstruction since 1950s. The text in the figure describes the median and 5th and 95th percentiles of the reconstruction model bootstrapped R^2, and median calibration validation statistics across the ensemble of 108 sequential leave-20-out cross-validated reconstruction. **(b.)** Range of reconstruction calibration-validation statistics computed for all 36 sequential leave-20-out model cross-validations for all 3 standardized chronology variants (2GR-RCS-SF, 3GR-RCS-TRAD, RCS and 3GRPSF). The median values for 108-member reconstruction ensemble are also shown. (i) CRSQ (calibration period coefficient of multiple determination), (ii) VRSQ (validation period square of the Pearson correlation), (iii) VRE (validation period reduction of error), and (iv) VCE (validation period coefficient of efficiency). **(c.)** Reconstruction of mean JJ temperature for western Mongolia between 1269-2004 C.E. The red triangles represent dates for 17 large tropical volcanic eruptions since 1269 C.E. from Toohey and Sigl, 2017. The dashed vertical line shows the year 1414, when EPS reaches 0.85.

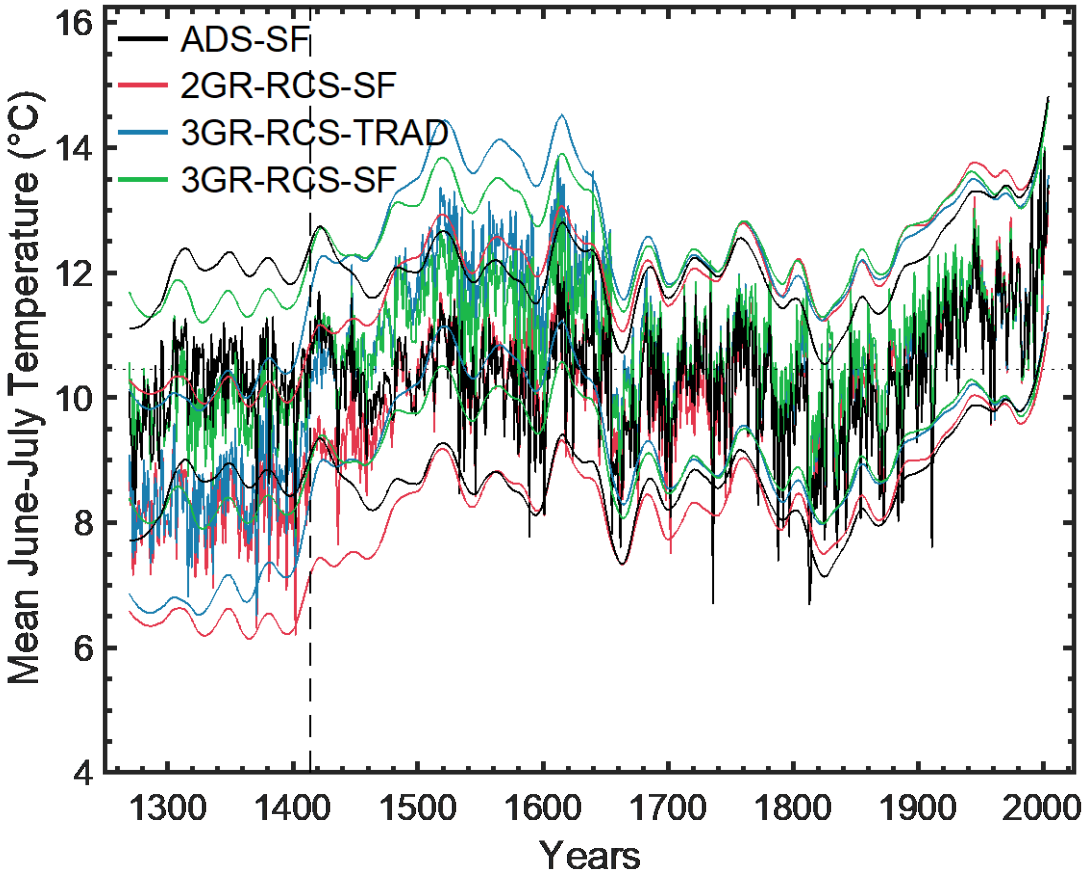

Figure S7. Comparison between reconstructions developed using four different standardized chronology variants, i. ADS-SF, ii. 2-GR-RCS-SF, ii. 3-GR-RCS-TRAD, and iii. 3GS-RCS-SF. Each reconstruction is calculated as the median of 36 leave-20-out sequential cross-validations. The confidence intervals for all four reconstructions are calculated as plus/minus twice its RMSQ and are smoothed with a 50-year loess filter for display. The dashed vertical line shows the year 1414, when EPS reaches 0.85.

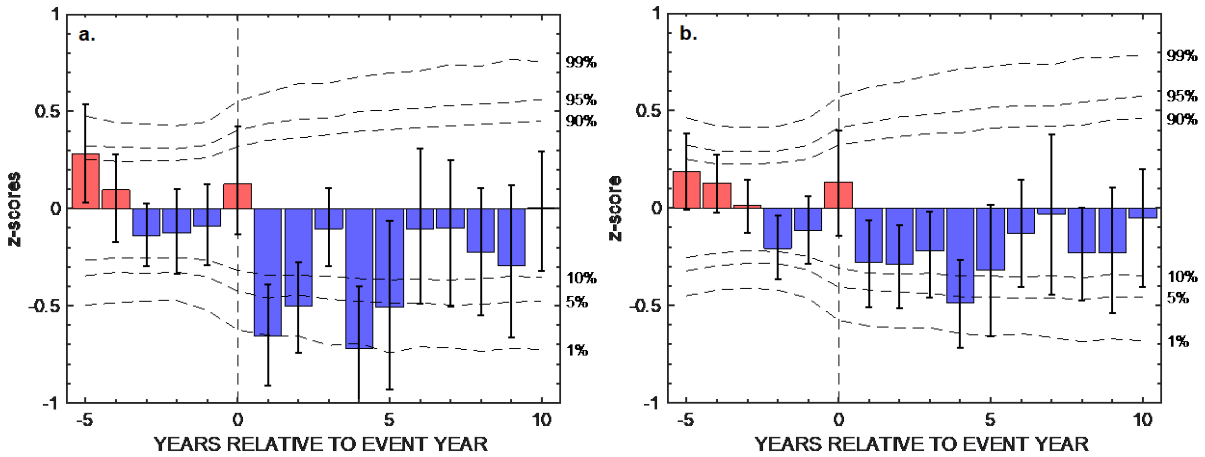

Figure S8 Same as Figure 3 (bottom panel) in the main text, except that SEA results are now shown as standardized anomalies (z-scores) for **a.)** the BUKK ADS-SF DBI chrnonology, and **b.)** the BUKK ringwidth (RW) chronology over the same time period (1269-2004 C.E.).

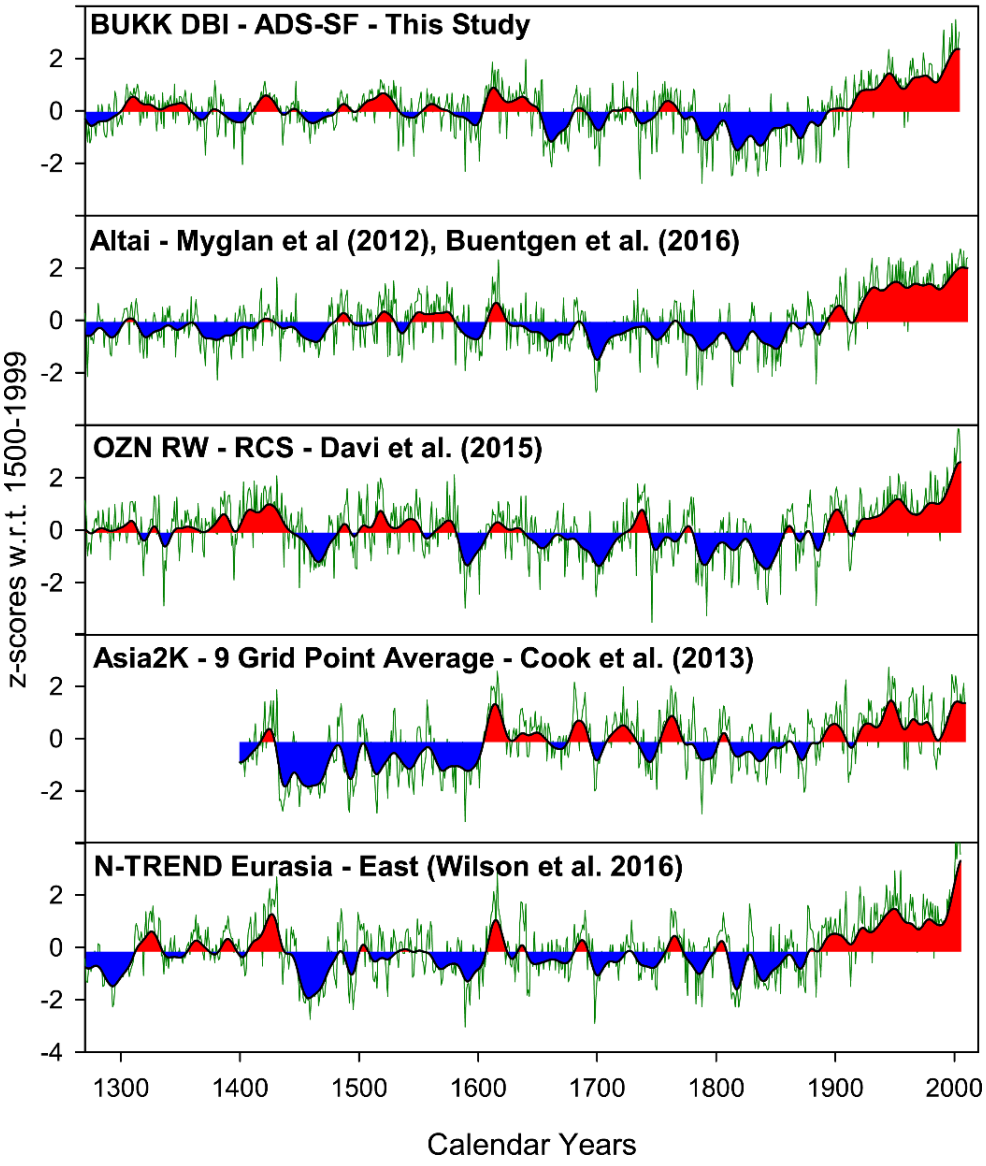

Figure S9. A summer temperature reconstruction comparison plot. Including, from top to bottom, BUKK (this study), an Altai Mountain reconstruction from China (Myglan et al., 2012; see also Büntgen et al., 2016), a ring-width based reconstruction from northern Mongolia (OZN - Davi et al., 2015), the mean of nine geographically related grids from the Asia 2K project (Cook et al. 2013), and a large-scale Eastern Eurasian tree-ring based composite record from NTREND (Wilson et al., 2016). The time-series were normalized to the 1500-1999 period and smoothed with a 25-year Gaussian filter.

	Model Name	Modeling Centre
1	ACCESS1-0	Centre for Australian Weather and Climate Research (CAWCR)
2	ACCESS1-3	
3	bcc-csm1-1	Beijing Climate Center, China Meteorological Administration (CMA)
4	CanESM2	Canadian Centre for Climate Modelling and Analysis
5	CCSM4	NCAR/UCAR Community Climate System Model
6	CESM1-BGC	
7	CESM1-CAM5	
8	CESM1-WACCM	
9	CNRM-CM5	Centre National de Recherches Meteorologiques / Centre Europeen de Recherche et Formation Avancees en Calcul Scientifique (CNRM/CERFACS)
10	CSIRO-Mk3-6-0	Commonwealth Scientific and Industrial Research Organisation
11	FIO-ESM	First Institute of Oceanography, State Oceanic Administration, China
12	GFDL-CM3	NOAA Geophysical Fluid Dynamics Laboratory
13	GFDL-ESM2G	
14	GFDL-ESM2M	
15	GISS-E2-R	NASA Goddard Institute for Space Studies
16	HadGEM2-CC	Met Office's Hadley Centre
17	HadGEM2-ES	
18	inmcm4	Institute for Numerical Mathematics
19	IPSL-CM5A-LR	Institut Pierre-Simon Laplace
20	IPSL-CM5A-MR	
21	IPSL-CM5B-LR	
22	MIROC-ESM	Atmosphere and Ocean Research Institute (The University of Tokyo), National Institute for Environmental Studies, and Japan Agency for Marine-Earth Science and Technology
23	MIROC-ESM-CHEM	
24	MIROC5	
25	MPI-ESM-LR	Max Planck Institute for Meteorology (MPI-M)
26	MRI-CGCM3	Meteorological Research Institute
27	NorESM1-M	Norwegian Climate Centre (NorClim)
28	NorESM1-ME	

Table S1. List of CMIP5 models (Taylor et al., 2012) used to derive projections of mean June-July temperature for the western Mongolia region for which we developed our temperature reconstruction. We used multiple ensemble members for each model. For each model, we first calculated the median temperature projection across ensemble members within each model, and only then calculated the median and interquartile range across models. We did this to ensure that each of the models are represented equally in the final multi-model ensemble estimate and to better compare 'future' and 'historical' projections where each model had different numbers of contributing ensemble members. The total number of ensemble members across all 28 models are, **i.** 110, historical period, 1850-2005, **ii.** 56, RCP4.5, 2006-2099, and **iii.** 71, RCP8.5, 2006-2099.

Five Coldest Years (°C)		**Five Coldest 5-year Period (°C)**		**Five Coldest 5-year Periods (°C) non overlapping**	
1813	6.69	1812-1816	7.78	1812-1816	7.78
1736	6.72	1813-1817	7.82	1660-1665	8.38
1189	6.78	1811-1816	8.15	1833-1838	8.38
1814	6.94	1814-1818	8.24	1869-1873	8.52
1788	7.39	1660-1665	8.38	1822-1826	8.62
Five Warmest Years (°C)		**Five Warmest 5-year Period (°C)**		**Five Warmest 5-year Periods (°C) non overlapping)**	
2001	13.95	2000-2004	12.94	2000-2004	13.41
1998	13.64	1998-2002	12.80	1994-1998	12.58
1991	13.47	1997-2001	12.80	1944-1948	12.17
2004	13.41	1999-2003	12.64	1962-1966	11.95
1996	13.16	1996-2000	12.64	1977-1981	11.88

Table S2: Coldest/warmest reconstructed year, five-year period, and non-overlapping five-year period.

GRID	LON	LAT
621	88.25	48.25
622	90.25	48.25
623	92.25	48.25
663	88.25	50.25
664	90.25	50.25
665	92.25	50.25
705	88.25	50.25
706	90.25	50.25
707	92.25	50.25

Table S3. Mean latitude and longitude of the nine Asia2K project grid cells from Western Mongolia (Cook et al., 2013).

Data Set S1. Our reconstruction R code and associated datasets have been made available as Supplementary Data 1.